

Cross-Category Functional Grasp Transfer

Rina Wu¹, Tianqiang Zhu¹, Xiangbo Lin¹, Yi Sun^{1*} *Member, IEEE*

Abstract—Generating grasps for a dexterous hand often requires numerous grasping annotations. However, annotating high DoF dexterous hand poses is quite challenging. Especially for functional grasps, the grasp pose must be convenient for subsequent manipulation tasks. This prompts us to explore how people achieve manipulations on new objects based on past grasp experiences. We find that when grasping new items, people are adept at discovering and leveraging various similarities between objects, including shape, layout, and grasp type. Considering this, we analyze and collect grasp-related similarity relationships among 51 common tool-like object categories and annotate semantic grasp representation for 1768 objects. These objects are connected through similarities to form a knowledge graph, which helps infer our proposed cross-category functional grasp synthesis. Through extensive experiments, we demonstrate that the grasp-related knowledge indeed contributed to achieving functional grasp transfer across unknown or entirely new categories of objects. We will publicly release the dataset and code to facilitate future research.

I. INTRODUCTION

With the rapid development of deep learning, the performance of dexterous grasp of robots has greatly improved through deep learning from a large amount of labeled grasps. However, annotating the high DoF grasps of multi-fingered robot hands on a large-scale objects is laborious and time-consuming. This prompts us to delve deeper into how humans can infer the various grasps of new or unseen objects only through the past grasping experience on limited amounts of objects. Such skill of grasp transfer is a hallmark of machine intelligence.

Previous studies in grasp transfer typically warp contact points on the source object to the target object through global and local shape similarities [1], coherent latent shape space [2] and dense corresponding descriptors [3]. More recently, several studies transfer labeled grasp poses [4] or hand-object touch code [5] from only one object to other ones within a category by the 3D-to-3D dense shape correspondence. That's based on the fact that objects of the similar shape in a category have similar grasps. Despite these recent successes in the transfer of grasping skills within similar objects, there is still no solution to the transfer of grasping skills to different categories of objects with significant differences in shape and function, which is the focus of this study.

To truly achieve human-level grasp skills for robot, we need to identify how a human grasp can be transferred

*This work was supported by the National Natural Science Foundation of China under Grants 62373075 and 61873046. (Corresponding author: Yi Sun)

¹ The authors are with the School of Information and Communication Engineering, Dalian University of Technology, Dalian, 116024, China. hswrn@mail.dlut.edu.cn, zhutq@mail.dlut.edu.cn, linxbo@dlut.edu.cn, lslwf@dlut.edu.cn

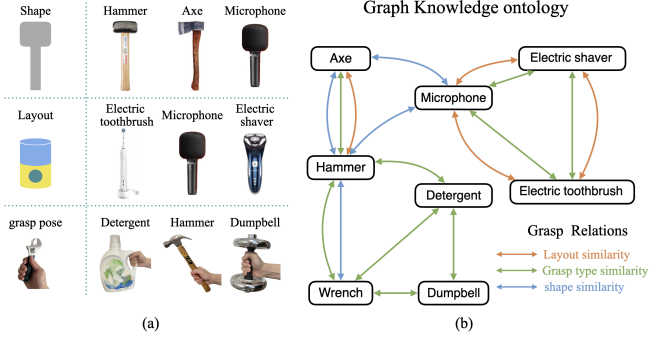


Fig. 1. (a) Three object attributes related to cross-category grasp transfer, as well as representative objects. (b) The part of knowledge graph ontology constructed based on the similarity of objects' three attributes.

across multiple categories of objects. In this work, we exploit the grasp-related semantic knowledge of objects to transfer grasps to new classes of objects. We start with 3 main observations. i) *Similar Shape*. Although the shape variance of objects in different categories is greater than that of objects in the same category, there is still shape similarity between some objects, as shown in Fig. 1 between a hammer and a microphone. ii) *Similar Layout*. For some different shapes of objects across categories, their layout of various parts is similar. For example, electric toothbrushes, microphones, and electric shavers have similar layout for functional grasp with the thumb placing on the switch and the remaining four fingers holding the body, as shown in Fig. 1. iii) *Similar Grasp Pose*. Some objects with significant shape variance may have same grasp pose, such as a detergent bottle and a hammer in Fig. 1. To encode these grasp relations between objects, we have established a grasp knowledge graph, as shown in Fig. 1(b), which can be used in our graph convolutional network-based grasp transfer framework.

It should be noted that this letter focuses on more complex functional grasp for post-grasp task manipulation. To this end, this work does not directly transfer grasp pose; instead, we transfer semantic touch code [6], a type of grasp representation that can be used for synthesizing functional grasps of objects. The reason behind this is that the touch code is easier to expand and has stronger generalization than hand-specific grasp pose and contact map [7], [8]. To better support cross-category functional grasp synthesis and establish new benchmarks for evaluating transfer performance, we increase object categories of the dataset in [6] from 18 to 51 and scale the number of objects from 129 to 1768. Moreover, we have designed a taxonomy for functional grasps to further ensure grasp synthesis. By applying grasping relationships to graph convolutional networks, the semantic representation of functional grasp can be transferred to different categories of objects and functional grasps of these objects can be



Fig. 2. The object part annotations.

ultimately optimized under the guidance of their transferred representations. To the best of our knowledge, this is the first effort in demonstrating functional grasp transfer for multi-fingered hand across different categories of objects. The contributions of this work can be summarized below:

- We propose 3 types of grasping relations across different categories of objects, and establish a grasp knowledge graph, which can be used in graph convolutional network for grasp transfer across categories.
- We not only scale the grasp dataset [6] in terms of object categories and numbers, but also add grasp types and grasping relations, which both gives a better benchmark for functional grasp synthesis and cross-category functional grasp transfer.
- We propose a novel cross-category functional grasp synthesis pipeline, which is composed of a touch code transfer framework based on graph convolutional networks and an optimization-based grasp synthesis module. Extensive experiments demonstrate that it can bridge the gap of functional grasp transfer to unseen and even completely new categories of objects.

II. RELATED WORK

Grasp transfer: There are many efforts being made to achieve grasp transfer based on global correspondence [9], local shape similarities [10]–[13], coherent latent shape space [2], or dense corresponding descriptors [14], [15]. However, these methods focus on how to grasp objects stably and do not explore more complex functional grasp. Recently, [5], [16] achieve intra-class functional grasp transfer through dense correspondences of object surface point, but this explicit surface point correspondence is challenging for cross-category objects with significant structural differences. In contrast, this letter summarizes the factors that people consider when reasoning about cross-category grasping. These factors are used to associate cross-category objects in the latent space for transfer of functional grasping across different categories.

Dexterous Manipulation Datasets: In recent years, numerous works [17], [18] have explored multi-fingered hand grasping, focusing primarily on stable grasp based on large-scale synthetic datasets [19]–[22]. However, for more practical and complex functional grasp, there are only a few datasets available. For example, [16], [23] record hand poses during real human-object interactions using visual sensors, [24] annotates grasp poses and contact affordance by the simulation software, and [7], [8] employ thermal camera to record contact map left on object surface after grasping. Moreover, [6] propose a semantic grasp representation, touch code, based on the object’s own components, which is universal for various dexterous hands. Nevertheless, all the above datasets lack support for cross-category functional

grasp transfer. In contrast, this letter proposes three types of inter-object similarities that establish associations among objects of different categories. Moreover, in terms of object diversity, our dataset includes 51 categories and 1768 objects, covering as many everyday tools as possible, surpassing most existing datasets. Our dataset can serve as the new benchmark for studies on functional grasp synthesis and cross-category grasp transfer.

III. METHOD

Cross-category functional grasp transfer is a challenging task. To address it, we have constructed grasp-related similarities across different categories of objects (Sec.A), grasp representation (touch code) for transfer (Sec.B), architecture for touch code transfer (Sec.C) and grasp synthesis based on the transferred touch code (Sec.D).

A. Grasp Similarities across Different Categories

To achieve human-level cross-category functional grasp synthesis, it is essential to comprehend the cross-category associations that support human inference for functional grasping across diverse object categories. To this end, we analyze the factors driving human grasp transfer across multiple categories of objects from three aspects: the global shape of objects, the object layout (i.e. spatial relative position of local parts), and the grasp type.

Shape similarity. The external shape of an object is its most easily observable attribute, and is also the most commonly used basis for grasp transfer [5]. To determine whether there is shape similarity between different categories of objects, we invited 15 participants to judge whether two categories are similar in shape by voting. If more than half of the votes consider the shapes to be similar, they are regarded as belonging to the same group. Subsequently, a new object category is compared with existing groups. If there is similarity, the new category is placed in the corresponding group; otherwise, it form a new group. This process continues until all 51 object categories are grouped.

Layout similarity. Although global shape similarity facilitates associations among cross-category objects, it falls short in capturing connections for objects requiring precise manipulation, like electric shavers and microphones. These objects’ cross-category functional grasp inference needs to further consider the local parts, especially the spatial relative positions between various parts (i.e., the layout of the object). For instance, electric shavers, microphones, and electric toothbrushes, despite their various shapes, share a consistent functional grasp pose due to the consistent relative position of touchable parts, like the switch on the middle of the handle (Fig. 2). In contrast, although a lighter also has a switch and a handle, its switch is located at the top of the handle, resulting in a different layout from a microphone. To collect the layout similarity between objects, we first annotate the touchable parts of 51 categories of objects, such as scissors with left and right handles or guns with a trigger and a handle, as shown in Fig. 2. Subsequently, participants grouped all object categories based on the annotated parts, and the grouping method was consistent with the Shape similarity.

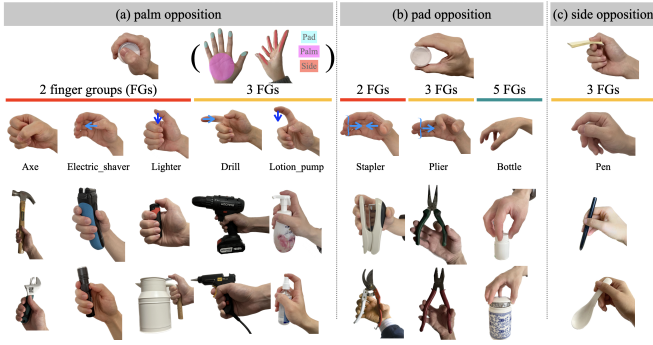


Fig. 3. The nine functional grasp types named after representative objects, each shows two examples.

Grasp type similarity. Shape and layout similarities are derived from an object-centric perspective to establish cross-category associations among objects. To further explore information applicable for cross-category grasp transfer, we analyze human-centric grasp types to group object categories. The human hand has a high degree of freedom, but it is redundant for grasping daily objects. This has led to many studies on the classification of grasp types, such as the commonly used 33 types of grasp taxonomy [25]. However, the current classification of grasp is mainly focused on static grasp, rather than the functional grasp of dynamic manipulation, such as the “drill” grasp type in Fig. 3 that cannot be classified into the 33 grasp types [25]. Considering that there is currently no taxonomy for functional grasp of dynamic manipulation, this work proposes the following classification criteria (taxonomy). Firstly, according to the type of opposition [26], functional grasps can be initially classified into three types: 1) palm opposition, wherein an object is grasped stably through the opposition between the palm and fingers, as illustrated in Fig. 3(a); 2) pad opposition, formed by two finger pads opposing each other (Fig. 3(b)); 3) side opposition, where the finger side is involved in the opposition, as illustrated by the pinching action in Fig. 3(c), which is accomplished by the upper side of the index finger and the thumb pad. Secondly, each opposition type can be further subdivided according to the finger movements. For instance, in the palm oppositions shown in Fig. 3(a), the five fingers gripping the ‘electric shaver’ (column 2) can be divided into 2 groups where the thumb manipulates the switch independently of the other four fingers and the remaining four fingers grip the handle. Similarly, the ‘drill’ type (column 4) can be divided into three finger groups: the thumb, the index finger, and the remaining three fingers. Moreover, the number of finger grouping of “lotion pump” type (column 5) is the same as “drill” type, but their index finger moves in different directions. Utilizing the aforementioned classification method, we subdivide the functional grasps of 51 categories of tool objects into 9 types, each showed with two representative object.

In summary, we establish associations among objects across categories from three aspects: global shape, object layout, and grasp type, which can collaborate effectively in facilitating grasp transfer as demonstrated in Section IV-A. Our objects are collected from 1) self-reconstructed

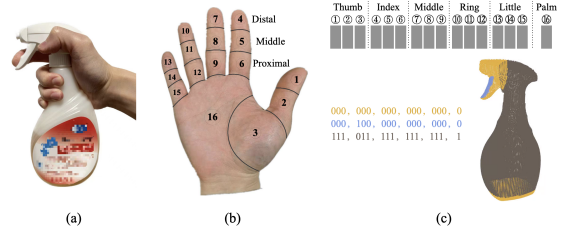


Fig. 4. (a) An example of functional grasp. (b) The 16 parts of human hands. (c) A example of the touch code.

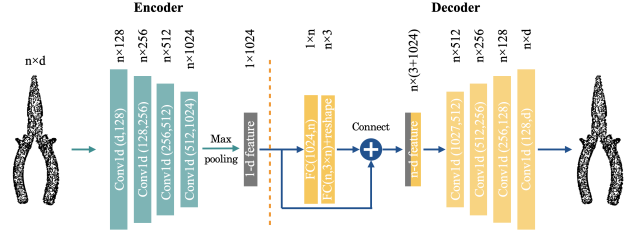


Fig. 5. The auto-encoder network (AENet).

through 3D scanner, 2) self-collected from online vendors, 3) some existing datasets, including ShapeNet [27], YCB [28], BigBIRD [29], KIT [30] and Grasp Database [31].

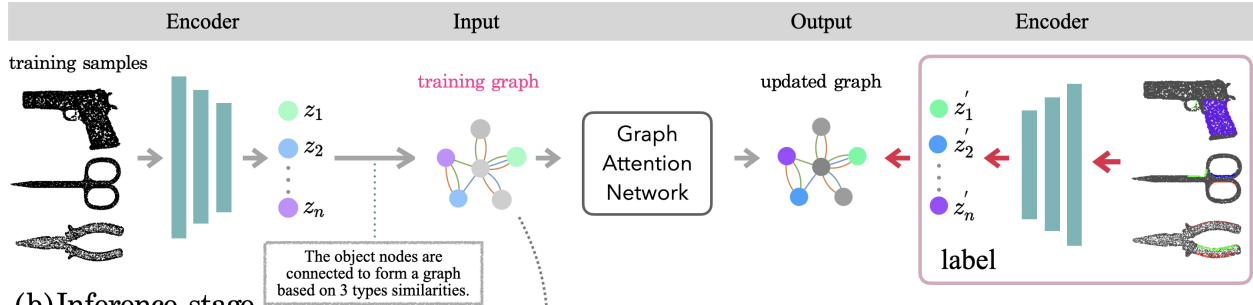
B. Grasp Representation for Transfer

With the three types of similarity mentioned above, this letter aims to transfer grasp on known objects to different categories of objects. Here, we choose to transfer touch code [6] because it is a semantic-based representation to specify which link of the dexterous hand should use to contact the object part in a functional grasp, so it is not limited to human hands or specific mechanical dexterous hands. These characteristics are consistent with our desired generality requirements. An example of touch code is shown in Fig. 4(c), where the sprayer bottle is divided into three parts, and each part has a 16-bit touch code to represent the correspondence between the object part and hand links (1 means that the hand link needs to touch this object part, and 0 means no touch). For example, the touch code of the blue trigger part is ‘000,100,000,000,000,0’, indicating that this part is usually touched by the distal index finger. Although Zhu et al. [6] have proposed a dataset about touch code, it contains insufficient categories and quantities of objects to support validation of cross-category touch code prediction. Therefore, we expand the dataset by augmenting the number of object categories from 18 to 51 and increasing the number of objects from 129 to 1768. This expanded dataset can not only serve as the basis for functional grasp synthesis, but also be used as a benchmark to validate the performance of cross-category touch code prediction.

C. Architecture for Touch Code Transfer

In the training phase, we first encode objects into the latent space. As shown in Fig. 5, we employ an auto-encoder (AENet) to obtain the one-dimensional feature for each object. The encoder compresses the object’s point cloud into a latent vector (referred to as the object feature), which is then reconstructed by the decoder back into the original input. We use the trained encoder to encode the training samples and obtain object features to build the knowledge graph. As

(a) Training stage



(b) Inference stage

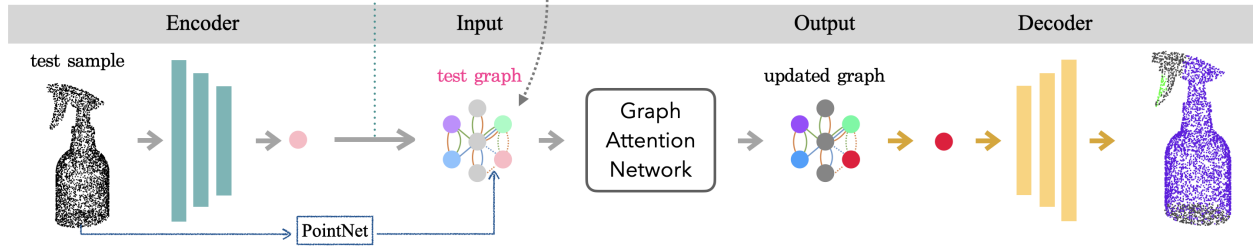


Fig. 6. (a) Training stage of our prediction framework. (b) Inference stage for new objects.

shown in Fig. 6, the encoded features of training samples are connected as nodes in a graph, and each edge between nodes corresponds to one of three types of similarity: shape, layout and grasp type similarity, resulting in the number of edges between nodes ranging from 0 (no correlation between two objects) to 3 (simultaneous existence of all three types of similarities). Of course, relying solely on the connection of latent features cannot achieve cross-category prediction. It is necessary for the feature to flow through the links of graph, so that each object node can gather information from related objects to enhance its own features. To accomplish this, we employ Graph Attention Network (GAT) [32] to update the constructed graph, where GAT is a common variant of Graph Convolutional Network that utilizes attention-based neighborhood aggregation. As shown in Fig. 6(a), we input the constructed graph into GAT, and the GAT would update the object feature in each node based on its neighboring nodes (i.e. the nodes that have similarity relationships with the current node). We supervise the updated feature in each node using the object’s touch code feature. To obtain the objects’ touch code features, we train another AEnet whose input is the object point cloud with each point concatenated with the 16-bit touch code. After the aforementioned training, GAT is capable of mapping object features to touch code features. However, It’s noteworthy that the trained GAT is not merely memorizing the touch code of the training samples; rather, the emphasis is on using inter-object similarities as reasoning bases to update each object feature, akin to human reasoning. This forms the foundation for predicting the touch code of new objects.

In the inference stage, we fully develop the GAT’s potential in handling dynamic graph. Specifically, we first link the test object feature into the graph used for training GAT. Here, we use point cloud classification networks to predict the link between objects (i.e. grouping). Taking grasp type similarity as an example, there are 9 functional grasp types in this

letter. We employ PointNet to forecast the grasp type for the test object. Next, as shown in Fig. 6(b), we use the trained GAT to update the new graph that includes a test node. In this process, the GAT essentially relies on three types of similarities to collect information from related objects for inferring the touch code feature of the new object. In this way, we can infer the touch code features of objects that are unseen or even completely new categories. The predicted touch code feature is then fed into the decoder to produce the point cloud with touch code for the test sample as shown in Fig. 6(b).

In general, we build the object associations in the latent space, and flexibly use GAT to handle dynamic graphs based on the three types of similarities to complete the prediction of new object’s touch code. Some details are as follows. Our algorithm runs on a 2080Ti GPU. To balance computational cost and prediction accuracy, we construct a total of 90 knowledge graphs to train the GAT, with each graph consisting of 360 nodes and each node corresponding to a randomly selected one of the 1167 training objects from 39 categories. In the inference phase, we first sample the point cloud of the test object and encode it into object feature, and then we connect the test object feature to a randomly one of 90 training knowledge graph, thus obtaining a test graph with 361 nodes. Finally, the test graph is input into the trained GAT to infer touch code feature, which will be decoded to generate the touch code of the test object. At this stage, we test a total of 601 objects from 49 classes, including 12 unseen classes to test cross-category prediction performance (Section IV-A).

D. Grasp Synthesis based on Transferred Touch Code

This section introduces how to synthesize the functional grasp $\langle J, T, R \rangle$ based on the transferred touch code O_c and the functional grasp type G , where J represents the joint angles of the dexterous hand, and R and T respectively denote the rotation and translation of the hand relative to the object.

TABLE I

THE MIOU RESULTS OF 10 COMBINATIONS, INCLUDING THE MIOU OF SEEN AND UNSEEN CATEGORIES OF OBJECTS. S=SHAPE, L=LAYOUT, G=GRASP TYPE, S+L MEANS THE SIMULTANEOUS USE OF SHAPE AND LAYOUT SIMILARITIES. AVG=AVERAGE MIOU.

Row	Relations	Seen					Unseen						
		pan	trigger_sprayer	pliers	stapler	Avg	flashlight	scrather	electric_teapot	twohead_wrench	spatula	paint_roller	Avg
1	No	90.88%	43.73%	23.57%	45.63%	58.59%	54.98%	59.88%	43.35%	54.09%	68.15%	42.65%	49.53%
2	Shape	97.11%	57.04%	45.12%	65.10%	68.87%	61.86%	65.76%	53.52%	66.21%	78.26%	59.21%	60.97%
3	Layout	94.07%	51.59%	45.43%	60.74%	65.23%	61.05%	64.15%	47.80%	71.82%	75.02%	57.07%	57.85%
4	Grasp type	95.87%	56.31%	39.53%	62.80%	67.53%	61.49%	65.09%	49.39%	55.28%	76.60%	62.36%	59.15%
5	S+L	97.36%	54.32%	45.62%	64.91%	70.32%	64.15%	66.10%	51.65%	84.26%	81.65%	62.54%	63.16%
6	S+G	97.22%	56.14%	45.61%	66.84%	71.93%	63.38%	68.01%	59.43%	78.85%	81.76%	71.61%	63.09%
7	L+G	97.41%	55.90%	49.48%	69.13%	73.20%	67.15%	68.92%	57.92%	73.78%	80.37%	73.31%	64.11%
8	S+L+G	97.56%	57.77%	45.15%	67.30%	73.89%	66.56%	71.93%	60.66%	88.53%	81.38%	77.15%	64.88%
9	PointNet	96.63%	55.68%	42.13%	63.21%	68.15%	63.65%	67.30%	56.03%	85.72%	77.93%	72.03%	60.43%
10	PointNet++	97.33%	55.39%	43.53%	65.19%	70.89%	65.11%	68.96%	58.26%	83.66%	79.25%	75.87%	62.01%

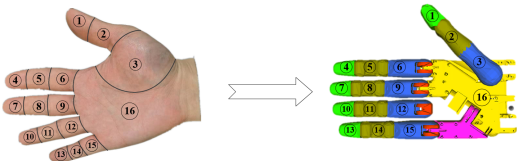


Fig. 7. Correspondence between human hand and Shadowhand.

To reduce the difficulty of optimizing the rotation variables in $SO(3)$, we first refer to [33] to provide a coarse rotation prior R_0 for the grasp synthesis, where the object point cloud feature and one candidate rotation prior (24 candidates in this letter, discretized along the main axes: $(x, y, z, -x, -y, -z)$) are input to the multilayer perceptron (MLP), and the MLP then outputs the joint probability density, which can be used to select the optimal rotation prior. In this way, the grasp synthesis can be modeled as $\mathcal{M} : \{O_c, G, R_0\} \Rightarrow \{J, R, T\}$, and here we use classical optimization method to synthesize functional grasp. Specifically, we chose the Shadowhand as the tested hand because it is currently the most dexterous robotic hand with the highest degrees of freedom, and optimizing it requires considering more variables, making it the most difficult to synthesize functional grasp. To synthesize functional grasp of an object, we initialize the dexterous hand pose with the functional grasp type we summarized, and design three objective functions based on the touch code to guide the dexterous hand to achieve functional grasp. To do so, we first need to align the functional grasp types and the touch code of human hand with the Shadowhand. To obtain these 9 initial grasp poses of the Shadowhand, we use kinematic mapping [34] to map the human grasp poses in functional grasp types to Shadowhand poses. While to make the touch code applicable to Shadowhand, we selected 16 links of Shadowhand corresponding to 16 parts of human hand as shown in Fig. 7. We design three objective functions by referring to the loss functions from prior work [5]. The first is the attraction function, which minimizes the distance between the links of the dexterous hand and the related object area specified by touch code (the area with touch code 1), such as the distance between the distal thumb and the flashlight switch. The second is the repulsion function, which serves to keep the links of the dexterous hand away from non-related object areas specified by touch code (the area with touch code 0). The third is the hand regularization function, which consists of two parts. The first part keeps the joint angles of the dexterous hand within a reasonable range,

and the second part prevents the fingers of the dexterous hand from colliding with each other. For detailed formulas, please refer to our prior work [5].

Our grasp optimization is mainly divided into two stages. The first stage only adjusts the translation and rotation of the hand, with an initial learning rate of 0.001 and a total of 100 rounds of optimization. The second stage mainly adjusts the joint angles of the dexterous hand, with an initial learning rate of 0.001, while the learning rates for translation and rotation are reduced to 0.0001, with a total of 200 optimization rounds. Thanks to the functional grasp types we proposed, this letter synthesizes higher-quality functional grasps using only classical optimization methods compared to existing network-based approaches [5]. The results of grasp synthesis are presented in Section IV-B.

IV. EXPERIMENT

A. Result of Similarity-based Touch Code Transfer

As described in Sec. III-C, our framework relies on three types of inter-object similarity to transfer the touch code of the training objects to new objects. To evaluate the effect of the touch code prediction, we tested a total of 49 object categories, including 12 unseen categories used to evaluate the cross-category prediction performance. Fig. 8 shows some of the test results, with seen categories on the left of the dashed line and the unseen categories on the right, where each object displays the touch code label (left) and prediction result (right) respectively. It can be observed that our framework not only predicts the touch codes of known categories effectively but also copes well with new categories. For example, the flashlight class highlighted in the red box was not involved in either the auto-encoder training or the GAT training, but associated with objects like electric shavers and electric toothbrushes through layout and grasp type similarities, enabling the flashlight to successfully achieve the touch code prediction of the head, switch, and body, without being misjudged as a hammer.

Moreover, Tab. I presents the quantitative results for touch code prediction, using the evaluation metric of mean intersection over union (mIoU). ‘Row-1’ represents the results of the baseline without using inter-object relationships, while ‘Row-8’ represents the results of our transfer framework when both training and testing use correct shape, layout, and grasp type similarities. By comparing ‘Row-1’ and

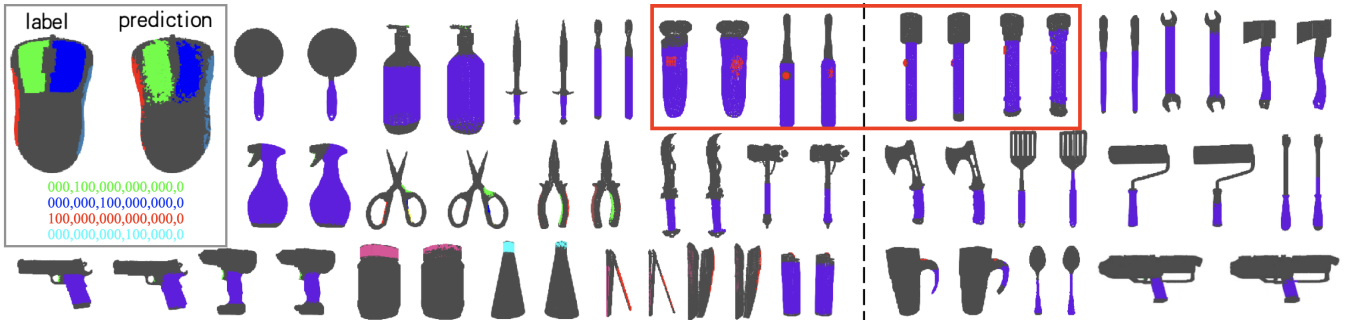


Fig. 8. The prediction result of the touch code, with known categories on the left side of the dashed line and new categories on the right. Taking the mouse in the top-left corner as an example, each object displays the touch code label (left) and the predicted touch code (right), with different color regions representing distinct touch codes.

‘Row-8’, it is evident that in both seen and unseen object categories, our prediction framework shows significant improvement than the baseline. We believe that when similarities are not used to associate objects, the network can only rely on its memory to handle some simple objects, such as 90.88% mIoU of the pans in ‘Row-1’. However, it is incapable of handling more complex objects, such as trigger sprayers, pliers, and flashlights, whose mIoUs of ‘Row-1’ (43.73%, 23.57%, 54.98%) are significantly lower than ‘Row-8’ (57.77%, 45.15%, 66.56%). In addition, based on the well-trained model of ‘Row-8’, we also evaluated the prediction effect when building test graphs based on PointNet and PointNet++ respectively, as shown in ‘Row-9’ and ‘Row-10’ (where the prediction accuracies for shape, layout, and grasp type similarity of PointNet and PointNet++ are 90.70%, 89.74%, 91.55% and 91.36%, 91.07%, 92.97%, respectively). As shown in Tab. I, the results of ‘Row-9’ and ‘Row-10’ are slightly inferior to ‘Row-8’.

Ablation Studies I . We conducted ablation studies on three similarities (rows 2-7), and some interesting conclusions can be drawn from these results: 1) Based on Avg mIoU of both seen and unseen categories, the results can be roughly divided into three groups, where the multi-relations groups (rows 5,6,7,8) outperform the single-relation groups (rows 2,3,4), while the no-relation group (row 1) has a significant gap with the other two groups. Therefore, it can be concluded that good knowledge transfer requires sufficient associations between objects. 2) The performance of ‘L+G’ (row 7) is better than ‘S+L+G’ (row 8) in some objects, such as the flashlight. We speculate that for flashlights, the association based on layout and grasp type similarity with objects like electric shavers is more crucial. In this case, introducing associations based on shape similarity with objects like hammers might lead to interference. Nevertheless, this does not imply that shape similarity is not important, as adding shape similarity for most objects can improve accuracy. This inspires us to explore how to intelligently adjust associations between objects to improve performance next.

Ablation Studies II. Although the above experiments demonstrate the effectiveness of our framework in predicting touch code, it may be due to the network has remembered the mapping rules from object initial features to the touch code features, rather than relying on associations to transfer

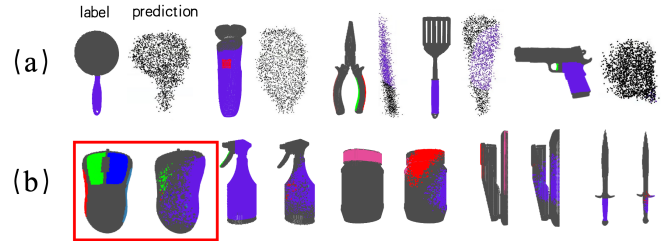


Fig. 9. (a) The predicted results of network on the graph that containing only test samples. (b) The prediction results when randomly connecting test sample to learned samples.

knowledge from previously learned samples to new objects. Therefore, we conducted the following two ablation experiments. 1) In our inference stage, the test object is connected to the training graph. To verify whether the learned objects in the training graph are necessary for predicting touch code, we generated a 360-node test graph containing only test objects, without using training graph as the connection. The prediction result is shown in Fig. 9(a), which reveals that the network is completely unable to handle these test samples, and even fails to retain the object structural information contained in the initial feature. 2) The second is to verify whether the similarities we proposed are effective in predicting the touch code. To achieve this, we randomly connect the test object to the previously learned objects in the training graph instead of using the correct associations. Fig. 9(b) shows the results. Taking the first mouse as an example, its result is completely incorrect. The reason is that the mouse is mistakenly associated with objects like guns and drills, leading to incorrect touch code prediction. The above two experiments illustrate that our prediction framework does not simply memorize the mapping between features, but actually achieves human-like reasoning, in which both reasonable inter-object associations and previously learned samples are crucial.

B. Functional Grasp Synthesis

As mentioned in Section III-D, we employ an optimization method based on predicted touch code and functional grasp type to synthesis functional grasp. It can be observed from the results in Fig. 10 that objects from both seen and unseen categories can achieve functional grasps effectively. For example, within the red box, the dexterous hand’s index and middle fingertip accurately land on the left and right buttons of the mouse, while the thumb, ring finger, and little

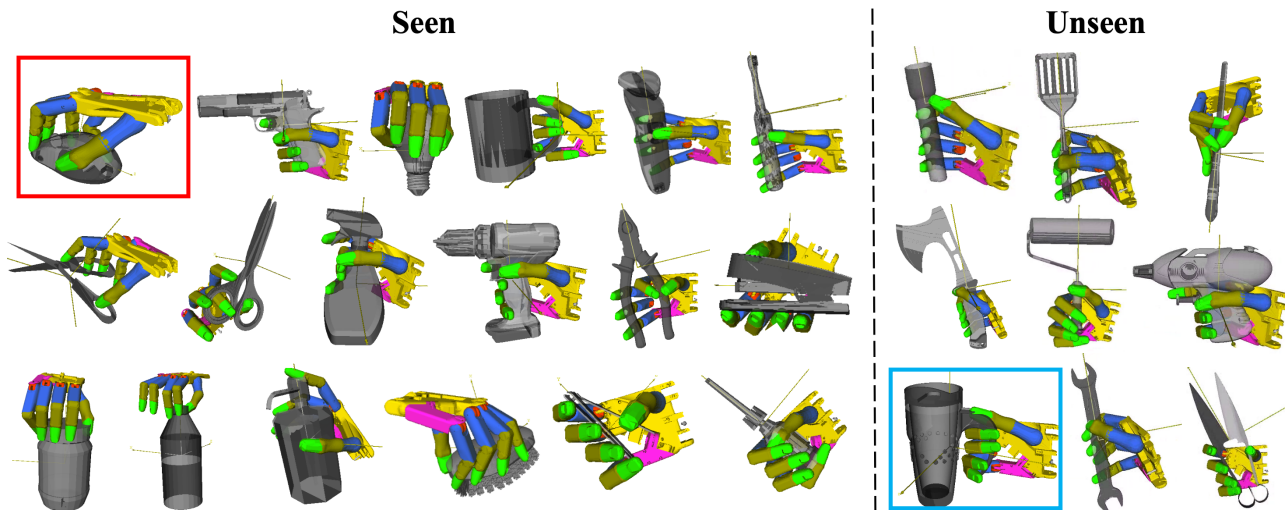


Fig. 10. Functional grasp synthesis results based on predicted touch code.

TABLE II
GRASP SUCCESS RATES OF OUR FUNCTIONAL GRASP.

Success Rate(%)	Seen				Unseen			
	drill	mouse	gun	sprayer	axe	electric.teapot	spoon	flashlight
Ours	85.7	70.0	63.2	76.5	66.7	66.7	75.0	83.3

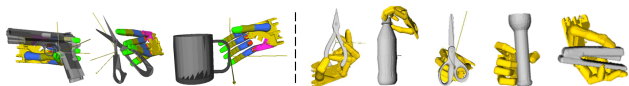


Fig. 11. Some grasp results of existing works. Left: [6]. Right: [36].

finger grasp the sides of the mouse. Another example is the electric teapot in the blue box, where the thumb presses the switch above the handle, and the remaining fingers hold the handle. Moreover, we use Isaac Gym [35] to calculate the success rate of grasps, where the object is considered to be grasped successfully if it does not fall within 10 seconds under random external force interference after being grasped. As indicated in the Tab. II, our method demonstrated a good success rate on both seen and unseen objects. For instance, in the case of cross-category grasp synthesis, the success rate for flashlights reached 83.3%.

In addition, it is not difficult to observe from Fig. 10 that our grasp poses are highly reasonable, approaching human-like grasps. This is not only attributed to the precise touch code prediction mentioned earlier but also benefited from the functional grasp types we proposed. Our functional grasp types can not only be used to build cross-category associations for touch code transfer, but also provide the reasonable initialization for dexterous hand in functional grasp synthesis. This enables the dexterous hand to make correct contact with the object in the right pose, as illustrated in the grasp of the second gun in Fig. 10, where the index finger accurately presses the trigger inside the loop. This advantage can be demonstrated through a comparison with two existing touch code-based functional grasp generation works [6], [36] that have not used our functional grasp types. As shown in Fig. 11, the grasping results of these two works exhibit unreasonable grasping poses, such as the grasp of the first gun, where the dexterous hand adopts a strange pose to strive for the correct contact, and the index finger approaches the

trigger in the opposite direction.

C. Comparison with Existing Works

In order to achieve cross-category grasp transfer for multi-fingered dexterous hands, some methods [1], [11] propose leveraging the local similarity of objects. However, these methods lack consideration for the overall structure and layout of objects, and can only achieve transfer of stable grasps for dexterous hands, rather than functional grasps needed for precise manipulation of objects such as flashlights and guns. The most relevant work to ours is [5], where they achieve functional grasp transfer within a category based on dense correspondences of surface points, achieving an 83.8% grasp success rate in the flashlight category. In comparison, this letter breaks through the intra-category constraints and achieves cross-category functional grasp transfer, with a success rate of 83.3% in the flashlight category.

V. CONCLUSIONS

To transfer the available functional grasps of objects to the other categories of objects, this letter analyzes the behavior of human grasping across categories and proposes three similarity relationships related to the grasp transfer. We propose the knowledge graph-based touch code transfer and optimization-based grasping synthesis framework, achieving cross-category functional grasp synthesis. It can be said that this letter creatively provides new insights and new benchmark for cross-category functional grasp transfer. However, for the convenience of reader comprehension and method implementation, this letter employs relatively basic models. Therefore, there is still considerable room for improvement in performance. In the future, we will improve the network to enhance its performance and design a more flexible structure to further achieve grasping across tasks. By dynamically adjusting the links between nodes, we aim to enable objects to have multiple uses for different tasks.

REFERENCES

- [1] N. Vahrenkamp, L. Westkamp, N. Yamanobe, E. E. Aksoy, and T. Asfour, "Part-based grasp planning for familiar objects," in *2016 IEEE-RAS 16th International Conference on Humanoid Robots (Humanoids)*. IEEE, 2016, pp. 919–925.
- [2] A. Simeonov, Y. Du, A. Tagliasacchi, J. B. Tenenbaum, A. Rodriguez, P. Agrawal, and V. Sitzmann, "Neural descriptor fields: Se (3)-equivariant object representations for manipulation," in *2022 International Conference on Robotics and Automation (ICRA)*. IEEE, 2022, pp. 6394–6400.
- [3] C. Liu, B. Fang, F. Sun, X. Li, and W. Huang, "Learning to grasp familiar objects based on experience and objects' shape affordance," *IEEE Transactions on Systems, Man, and Cybernetics: Systems*, vol. 49, no. 12, pp. 2710–2723, 2019.
- [4] H. Wen, J. Yan, W. Peng, and Y. Sun, "Transgrasp: Grasp pose estimation of a category of objects by transferring grasps from only one labeled instance," in *European Conference on Computer Vision (ECCV)*, 2022, pp. 445–461.
- [5] R. Wu, T. Zhu, W. Peng, J. Hang, and Y. Sun, "Functional grasp transfer across a category of objects from only one labeled instance," *IEEE Robotics and Automation Letters*, vol. 8, no. 5, pp. 2748–2755, 2023.
- [6] T. Zhu, R. Wu, J. Hang, X. Lin, and Y. Sun, "Toward human-like grasp: Functional grasp by dexterous robotic hand via object-hand semantic representation," *IEEE Transactions on Pattern Analysis and Machine Intelligence*, 2023.
- [7] S. Brahmabhatt, C. Ham, C. C. Kemp, and J. Hays, "Contactdb: Analyzing and predicting grasp contact via thermal imaging," in *Proceedings of the IEEE/CVF conference on computer vision and pattern recognition*, 2019, pp. 8709–8719.
- [8] S. Brahmabhatt, A. Handa, J. Hays, and D. Fox, "Contactgrasp: Functional multi-finger grasp synthesis from contact," in *2019 IEEE/RSJ International Conference on Intelligent Robots and Systems (IROS)*. IEEE, 2019, pp. 2386–2393.
- [9] D. Rodriguez and S. Behnke, "Transferring category-based functional grasping skills by latent space non-rigid registration," *IEEE Robotics and Automation Letters*, vol. 3, no. 3, pp. 2662–2669, 2018.
- [10] A. Tekden, M. P. Deisenroth, and Y. Bekiroglu, "Grasp transfer based on self-aligning implicit representations of local surfaces," *IEEE Robotics and Automation Letters*, vol. 8, no. 10, pp. 6315–6322, 2023.
- [11] M. S. Kopicki, D. Belter, and J. L. Wyatt, "Learning better generative models for dexterous, single-view grasping of novel objects," *The International Journal of Robotics Research*, vol. 38, no. 10-11, pp. 1246–1267, 2019.
- [12] Ü. R. Aktaş, C. Zhao, M. Kopicki, and J. L. Wyatt, "Deep dexterous grasping of novel objects from a single view," *International Journal of Humanoid Robotics*, vol. 19, no. 02, p. 2250011, 2022.
- [13] H. Geng, H. Xu, C. Zhao, C. Xu, L. Yi, S. Huang, and H. Wang, "Gapartnet: Cross-category domain-generalizable object perception and manipulation via generalizable and actionable parts," in *Proceedings of the IEEE/CVF Conference on Computer Vision and Pattern Recognition*, 2023, pp. 7081–7091.
- [14] C.-Y. Chai, K.-F. Hsu, and S.-L. Tsao, "Multi-step pick-and-place tasks using object-centric dense correspondences," in *2019 IEEE/RSJ International Conference on Intelligent Robots and Systems (IROS)*. IEEE, 2019, pp. 4004–4011.
- [15] S. Yang, W. Zhang, R. Song, J. Cheng, and Y. Li, "Learning multi-object dense descriptor for autonomous goal-conditioned grasping," *IEEE Robotics and Automation Letters (RA-L)*, vol. 6, no. 2, pp. 4109–4116, 2021.
- [16] L. Yang, K. Li, X. Zhan, F. Wu, A. Xu, L. Liu, and C. Lu, "Oakink: A large-scale knowledge repository for understanding hand-object interaction," in *Proceedings of the IEEE/CVF Conference on Computer Vision and Pattern Recognition*, 2022, pp. 20953–20962.
- [17] M. Van der Merwe, Q. Lu, B. Sundaralingam, M. Matak, and T. Hermans, "Learning continuous 3d reconstructions for geometrically aware grasping," in *2020 IEEE International Conference on Robotics and Automation (ICRA)*. IEEE, 2020, pp. 11 516–11 522.
- [18] Y. Xu, W. Wan, J. Zhang, H. Liu, Z. Shan, H. Shen, R. Wang, H. Geng, Y. Weng, J. Chen *et al.*, "Unidexgrasp: Universal robotic dexterous grasping via learning diverse proposal generation and goal-conditioned policy," in *Proceedings of the IEEE/CVF Conference on Computer Vision and Pattern Recognition*, 2023, pp. 4737–4746.
- [19] W. Wei, D. Li, P. Wang, Y. Li, W. Li, Y. Luo, and J. Zhong, "Dvvg: Deep variational grasp generation for dextrous manipulation," *IEEE Robotics and Automation Letters (RA-L)*, vol. 7, no. 2, pp. 1659–1666, 2022.
- [20] M. Liu, Z. Pan, K. Xu, K. Ganguly, and D. Manocha, "Generating grasp poses for a high-dof gripper using neural networks," in *2019 IEEE/RSJ International Conference on Intelligent Robots and Systems (IROS)*. IEEE, 2019, pp. 1518–1525.
- [21] J. Varley, J. Weisz, J. Weiss, and P. Allen, "Generating multi-fingered robotic grasps via deep learning," in *2015 IEEE/RSJ international conference on intelligent robots and systems (IROS)*. IEEE, 2015, pp. 4415–4420.
- [22] V. Mayer, Q. Feng, J. Deng, Y. Shi, Z. Chen, and A. Knoll, "Ffhnet: Generating multi-fingered robotic grasps for unknown objects in real-time," in *2022 International Conference on Robotics and Automation (ICRA)*. IEEE, 2022, pp. 762–769.
- [23] Y. Liu, Y. Liu, C. Jiang, K. Lyu, W. Wan, H. Shen, B. Liang, Z. Fu, H. Wang, and L. Yi, "Hoi4d: A 4d egocentric dataset for category-level human-object interaction," in *Proceedings of the IEEE/CVF Conference on Computer Vision and Pattern Recognition*, 2022, pp. 21 013–21 022.
- [24] J. Jian, X. Liu, M. Li, R. Hu, and J. Liu, "Affordpose: A large-scale dataset of hand-object interactions with affordance-driven hand pose," in *Proceedings of the IEEE/CVF International Conference on Computer Vision*, 2023, pp. 14 713–14 724.
- [25] T. Feix, J. Romero, H.-B. Schmiebmayer, A. M. Dollar, and D. Kragic, "The grasp taxonomy of human grasp types," *IEEE Transactions on human-machine systems*, vol. 46, no. 1, pp. 66–77, 2015.
- [26] T. Iberall, "Human prehension and dexterous robot hands," *The International Journal of Robotics Research*, vol. 16, no. 3, pp. 285–299, 1997.
- [27] A. X. Chang, T. Funkhouser, L. Guibas, P. Hanrahan, Q. Huang, Z. Li, S. Savarese, M. Savva, S. Song, H. Su *et al.*, "Shapenet: An information-rich 3d model repository," *arXiv preprint arXiv:1512.03012*, 2015.
- [28] B. Calli, A. Walsman, A. Singh, S. Srinivasa, P. Abbeel, and A. M. Dollar, "Benchmarking in manipulation research: The ycb object and model set and benchmarking protocols," *arXiv preprint arXiv:1502.03143*, 2015.
- [29] A. Singh, J. Sha, K. S. Narayan, T. Achim, and P. Abbeel, "Bigbird: A large-scale 3d database of object instances," in *2014 IEEE international conference on robotics and automation (ICRA)*. IEEE, 2014, pp. 509–516.
- [30] A. Kasper, Z. Xue, and R. Dillmann, "The kit object models database: An object model database for object recognition, localization and manipulation in service robotics," *The International Journal of Robotics Research*, vol. 31, no. 8, pp. 927–934, 2012.
- [31] D. Kappler, J. Bohg, and S. Schaal, "Leveraging big data for grasp planning," in *2015 IEEE international conference on robotics and automation (ICRA)*. IEEE, 2015, pp. 4304–4311.
- [32] P. Velickovic, G. Cucurull, A. Casanova, A. Romero, P. Liò, and Y. Bengio, "Graph attention networks," in *6th International Conference on Learning Representations, ICLR 2018, Vancouver, BC, Canada, April 30 - May 3, 2018, Conference Track Proceedings*. OpenReview.net, 2018.
- [33] K. A. Murphy, C. Esteves, V. Jampani, S. Ramalingam, and A. Makadia, "Implicit-pdf: Non-parametric representation of probability distributions on the rotation manifold," in *Proceedings of the 38th International Conference on Machine Learning*, ser. Proceedings of Machine Learning Research, M. Meila and T. Zhang, Eds., vol. 139. PMLR, 18–24 Jul 2021, pp. 7882–7893.
- [34] S. Li, X. Ma, H. Liang, M. Görner, P. Ruppel, B. Fang, F. Sun, and J. Zhang, "Vision-based teleoperation of shadow dexterous hand using end-to-end deep neural network," in *2019 International Conference on Robotics and Automation (ICRA)*. IEEE, 2019, pp. 416–422.
- [35] V. Makoviychuk, L. Wawrzyniak, Y. Guo, M. Lu, K. Storey, M. Macklin, D. Hoeller, N. Rudin, A. Allshire, A. Handa *et al.*, "Isaac gym: High performance gpu based physics simulation for robot learning," in *Thirty-fifth Conference on Neural Information Processing Systems Datasets and Benchmarks Track (Round 2)*, 2021.
- [36] Y. Zhang, J. Hang, T. Zhu, X. Lin, R. Wu, W. Peng, D. Tian, and Y. Sun, "Functionalgrasp: Learning functional grasp for robots via semantic hand-object representation," *IEEE Robotics and Automation Letters*, vol. 8, no. 5, pp. 3094–3101, 2023.